Decisions in Economics and Finance
https://doi.org/10.1007/s10203-025-00531-y

The discrete solow model with time-to-build

Akio Matsumoto[1,2] · **Márk Molnár**[3] · **Ferenc Szidarovszky**[4]

Received: 29 December 2024 / Accepted: 21 June 2025

Abstract
This study reformulates the discrete-time Solow economic growth model by incorporating time delays and re-evaluates capital accumulation in two distinct frameworks: one in which the population growth rate is constant (either positive or negative) and another in which it varies over time. The analysis demonstrates that: (i) the stability conditions under delay remain valid; (ii) the delayed Solow model exhibits cyclic fluctuation through a Neimark-Sacker bifurcation when the time delay is sufficiently long and the labor force growth rate is low, including cases of negative growth; and (iii) the stability of the system is highly sensitive to the specification of the labor force dynamics. As a direction for future research, it would be interesting to replace the Cobb-Doglas production function with a Constant Elasticity of Substitution (CES) production function as empirical evidence suggests that the elasticity of substitution is typically less than one.

Keywords Time-to-build · Discrete Solow model · Stability conditions · Negative and Non-constant population growth rates

The authors are grateful to two reviewers for helpful comments and suggestions. The first author highly acknowledges the financial supports from the Japan Society for the Promotion of Science (Grant-in-Aid for Scientific Research (C), 20K01566, 24K04789) and 2023-24 Collaborate Research A of the Research Institute of Economic Science, Nihon University. We appreciate K. Sakurai (Rissho University) and Y. Ishida (Kyoto University) for fruitful discussions on the population growth rates in the OECD countries. The usual disclaimers apply.

✉ Akio Matsumoto
akiom@tamacc.chuo-u.ac.jp

Márk Molnár
Molnar.Mark@gtk.elte.hu

Ferenc Szidarovszky
szidarka@gmail.com

1 Department of Economics, Chuo University, 742-1, Higashi-Nakano, Hachioji, Tokyo 192-0393, Japan

2 CIAS, Corvinus University, Budapest, Fövám tér 8 1093, Hungary

3 Faculty of Economics, Eötvös Loránd University, Budapes, Rákóczi út 7 1088, Hungary

4 Department of Mathematics, Corvinus University, Budapest, Fövám tér 8 1093, Hungary

Published online: 07 July 2025

Mathematics Subject Classification C62 · E32 · O41

1 Introduction

Solow (1956) pioneered a dynamic model of macroeconomics that provides a theoretical explanation for understanding long-run economic growth. According to this model, intensive capital and output monotonically converge to the steady states, while extensive capital and output follow a balanced growth path determined by the population growth rate. In this study, we extend the discrete-time Solow model in three important ways. First, we introduce a time delay to account for the inherent time-consuming nature of economic activities. In the standard Solow model, economic growth is driven by two exogenously given factors: the saving rate which influences capital accumulation and the population growth rate which determines the available labor force. However, the saving rate may depend on income and the interest rates, and a constant growth rate is a reasonable assumption only in short-term analyses. While the reconsideration of the constant saving rate is typically addressed through the development of the Ramsey model, our focus is on re-evaluating the assumption of a constant population growth rate. Furthermore, empirical demographic evidence particularly from developed countries suggests that population decline is an inevitable trend. Hence, to assess the implications of such demographic shifts we examine the long-run dynamics of the Solow model under scenarios where population growth is negative and non-constant. Specifically, we re-evaluate the long-run economic growth within two distinct frameworks: one in which population growth is exogenously given (either positive or negative) and another in which it is endogenously determined .

In this study, we adopt the discrete-time Solow model. When a difference equation describes a macroeconomic dynamic model, it inherently implies a "delay" in production as production processes require at least one period to be completed. Introducing an explicit "time delay" extends this concept by assuming that new capital construction requires more than a single time period. In dynamic analysis, both continuous-time and discrete-time versions of the Solow model can capture long-run economic growth.[1] Kalecki (1935) was the first to demonstrate that time delays in capital production, implementation and installation can serve as a source of cyclic fluctuations in a continuous-time macroeconomic dynamic model. The literature on delay Solow models in continuous-time is extensive with notable contributions from Zak (1999), Guerrini et al. (2019), and Matsumoto and Szidarovszky (2023), among others. More recently, Matsumoto and Szidarovszky (2025) reformulated the intensive capital accumulation equation as a delay differential equation with delay-dependent coefficients and identified conditions under which the interaction between time delays and the population growth rate induces growth cycles. On the other hand, Day (1982) demonstrated that the discrete-time Solow model can generate complex dynamics including chaotic behavior when strong nonlinearity arises from pollution effects in

[1] There is a long controversy regarding a choice of continuous-time or discrete-time for constructing a dynamic model. Chaos theory demonstrates the advantage of discrete models for generating complicated fluctuations observed in actual economic data. Gandolfo (1997, Section 27) summarizes the advantages of continuous models.

the production function. Similarly, Kydland and Prescott (1982) explained the emergence of cyclical fluctuations in a discrete-time equilibrium growth model with time delays. In the presence of time-to-build effects, the resulting capital accumulation equation takes the form of a high-order difference equation in intensive capital. In this study, we investigate the conditions under which cyclic dynamics emerge within this framework.

Since the 1950s, demographics have undergone significant transformations, with increasing concerns about population aging and decline. In a growing number of countries, fertility rates have remained persistently low for several decades – rising from 14 countries in 1980 to 63 today, according to the World Population Prospects (2024). As a natural consequence, many countries have already reached their peak population and are experiencing continued population decline. Population growth rate is a key driver of economic expansion, yet recent trends indicate a shift toward negative growth in many regions. Figure 1 illustrates the relationship between the logarithm of total population and population growth rate across OECD countries.[2] The vertical axis represents countries with populations between 5.5 million and 1 billion, while the horizontal axis spans growth rates from -1.5% to 2%. Each country is labeled with a three-letter country code and different geographic regions are represented using distinct colors: Australia and Oceania (blue), Central America (orange), Europe (blue), the Middle East (black), North America (light blue), South America (magenta), and South Asia (red). The plane is divided into two zones: a light-green area indicating negative growth rates and a light-red area for positive growth rates. The data reveal that large population countries, such as Germany (84 million), Italy (60 million), and Poland (39 million) are already experiencing negative population growth. Similarly, countries with near-zero but positive growth rates, such as France (0.2%, 69 million), South Korea (0.21%, 52 million) and Spain (0.12%, 47 million) are expected to shift into negative growth in the near future, given that their fertility rates have remained below replacement level for several years. Japan (123 million), another country with a large population is already experiencing negative growth, driven by a declining birth rate and an aging population due to increasing life expectancy. The decline in fertility rates across developing nations is frequently attributed to advancements in education and health care.[3]

Various modified versions of the Solow model have explored economic growth under non-constant population growth. Brianzoni et al. (2007, 2009) extended the standard model by replacing the Cobb-Douglas production function with the Constant Elasticity of Substitution (CES) function, introducing two distinct groups of agents - workers and shareholders - with different but constant saving rates. They further assumed that population growth follows either the Beverton-Holt equation or the logistic equation, leading to dynamic systems exhibiting a range of behaviors from cyclic fluctuations to chaotic dynamics. Brida and Pereyra (2008) adopted a generic population law characterized by two key properties: a strictly increasing and bounded population size and a strictly decreasing population growth rate. Their anal-

[2] We obtain those demographic data from CIA The World Factbook, 2024.

[3] In standard economic growth theory, the population growth rate is typically assumed to be positive. However, the demographic evidence observed in the light-green area of Figure 1 challenges this assumption, highlighting the need to reconsider economic models in the context of negative population growth.

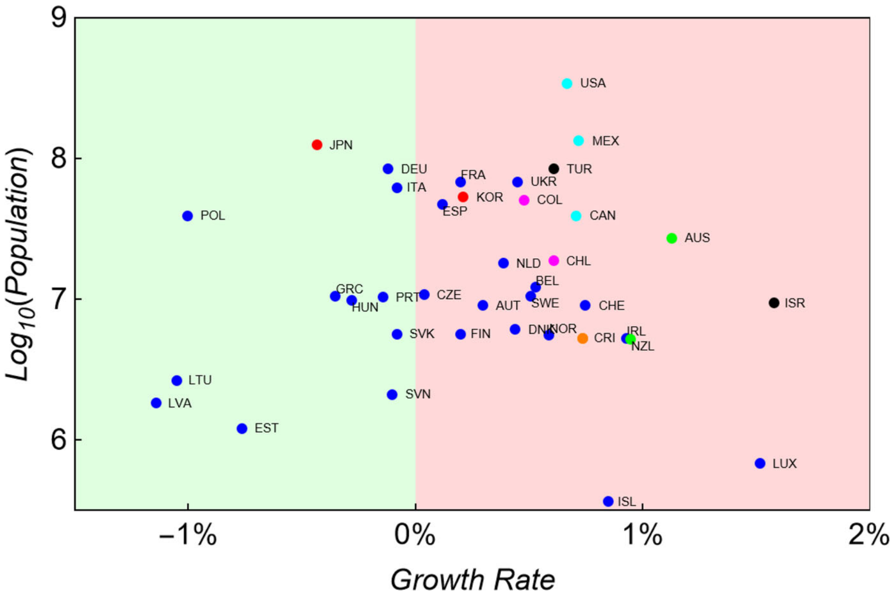

Fig. 1 Scatter plot of the population growth rate and the total number of population in the OECD countries

ysis demonstrated the stability of the steady state under these conditions. Tramontana et al. (2015) considered a Leontief production function, different savings rates for two types of agents, and logistic labor force growth. Their results revealed a cascade of flip bifurcations in a one-dimensional map and a sequence of pitchfork and flip bifurcations in a two-dimensional map, highlighting the complexity of economic dynamics under these assumptions.

In this study we will also examine the implications of negative or non-constant population growth for long run economic growth. The remainder of the paper is structured as follows. Section 2 provides a brief summary of the discrete Solow model without delays. Section 3 introduces a production delay under constant population growth rate and is divided into two subsections: the first derives delay stability conditions, while the second presents numerical examples illustrating the emergence of cyclic fluctuation. Section 4 explores two special cases: the first subsection demonstrates that production delay alone does not destabilize the system, while the second shows that depreciation delay induces instability. Section 5 extends the delay analysis to scenarios with non-constant population growth. Section 6 concludes the study.

2 Solow model: brief review

In this section, we provide a brief review the long-run dynamics of the Solow growth model. The economy produces a single output $Y(t)$ using two factors, capital $K(t)$ and labor $L(t)$ at date t. For analytical simplicity and consistency with standard economic modelling, we adopt three key assumptions. First, the production function follows the

Cobb-Douglas specification, which transforms the two inputs into output as follows:

$$Y(t) = K^{\alpha}(t)L^{1-\alpha}(t) \text{ with } 0 < \alpha < 1 \tag{1}$$

where there is no technical progress assumed. Second, gross investment is equal to aggregate savings which is a fixed fraction s of gross output,

$$I(t) = sY(t) \text{ with } 0 < s < 1.$$

The change in the extensive capital stock is equal to gross investment minus the capital depreciation, denoted as $\delta K(t)$ where δ represents the depreciation with $0 < \delta < 1$. Given the assumptions above, the evolution of extensive capital is expressed by

$$K(t+1) - K(t) = sK^{\alpha}(t)L^{1-\alpha}(t) - \delta K(t). \tag{2}$$

Lastly, the labor force is assumed to grow at a constant rate, n where $n \neq 0$,

$$L(t+1) = (1+n)L(t) \tag{3}$$

Since full employment is assumed in the Solow model, population and labor force are considered mutually substitutable. The fundamental question posed by Solow (1956) is how the economy evolves, given the initial values of capital and labor, denoted as K_0 and L_0 under the specified conditions. To address this question, we first define new variables, the per-capita capital and per-capita output,

$$k(t) = \frac{K(t)}{L(t)} \text{ and } y(t) = \frac{Y(t)}{L(t)}.$$

Next, we divide both sides of Equation (2) by $L(t)$ to derive the intensive (i.e., per-capita) capital accumulation equation,

$$k(t+1) = \frac{1}{1+n}k(t) + \frac{s}{1+n}k^{\alpha}(t) - \frac{\delta}{1+n}k(t). \tag{4}$$

This equation describes capital accumulation over time, given the initial per-capita capital, $k_0 = K_0/L_0$, which is exogenously determined. Equation (4) is often referred to as the *fundamental dynamic equation* in the neoclassical growth theory. To derive the steady state, we impose the condition, $k_* = k(t+1) = k(t)$, and substitute it into Equation (4),

$$k_* = \left(\frac{s}{n+\delta}\right)^{\frac{1}{1-\alpha}}. \tag{5}$$

Population growth rates exhibit considerable variation across countries, with a broad range of −2% to 5% encompassing the majority of nations globally. As illustrated in Figure 1, a narrower range of −1% to 2% characterizes most OECD countries. This study considers both positive and negative population growth scenarios. In contrast, the depreciation rate is estimated to be at least 10%, implying that capital stock depletion occurs at a relatively high rate. Consequently, it is reasonable to impose the following condition on n to ensure that the steady-state capital stock k remains positive even in cases where n assumes negative values:

Assumption 1 $|n| < \delta$

Equation (4) presents a first-order nonlinear difference equation in $k(t)$. The function is both increasing and strictly concave, properties that ensures the asymptotic stability of the steady-state capital stock k_*,

$$\frac{dk(t+1)}{dk(t)} = \frac{\alpha s}{1+n} k^{\alpha-1}(t) + \frac{1-\delta}{1+n} > 0$$

and

$$\frac{d^2k(t+1)}{dk(t)^2} = -\frac{\alpha(1-\alpha)s}{1+n} k^{\alpha-2}(t) < 0.$$

The key findings derived from the discrete-time Solow model are summarized as follows. Given the asymptotic stability of k_*, the intensive capital stock $k(t)$ and output $y(t)$ converge to their respective steady states values, denoted as k_* and $y_* = k_*^{\alpha}$,

$$\lim_{t\to\infty} k(t) = k_* \text{ and } \lim_{t\to\infty} y(t) = y_*.$$

Since the labor force grows at constant rate n, the growth rates of the extensive variables, capital $K(t)$ and output $Y(t)$, asymptotically approach the exogenously given growth rate n for any positive initial points (i.e., $K_0 > 0$ and $Y_0 > 0$) as time progresses,[4]

$$\lim_{t\to\infty} \frac{K(t+1) - K(t)}{K(t)} = \lim_{t\to\infty} \frac{Y(t+1) - Y(t)}{Y(t)} = n.$$

Although the population growth rate is typically assumed to be positive, convergence remains valid even in the case of a negative growth rate provided that Assumption 1 holds. This result highlights the potential for economic decline in scenarios where population contraction occurs.

3 The Delayed solow model with a constant *n*

In this section, we introduce a time delay into the dynamic equation (2) to examine its impact on stability properties. The inclusion of a time delay accounts for the lag in the production and implementation of capital goods, reflecting the multi-period process required to build new capital. The delay, referred to as a production delay, characterizes

[4] In the steady state, these extensive variables are in a balanced growth path in which the growing at rate is n.

a time-to-build framework within the Solow model. This section is structured as follows: the first subsections analyzes the stability conditions under the introduced delay, while the second subsection explores the emergence of complex dynamic behavior resulting from the delay mechanism

3.1 Delay stability conditions

Under a constant population growth rate and a multi-period delay $t-\tau$ where $\tau \geq 1$, the extensive capital accumulation Eq. (2) is modified as follows:

$$K(t+1) - K(t) = sK(t-\tau)^{\alpha} L(t)^{1-\alpha} - \delta K(t-\tau) \tag{6}$$

where $K(t-\tau)$ is the capital available at time t due to delay τ. Dividing both sides of Equation (6) by $L(t)$ yields

$$\frac{K(t+1)}{L(t+1)}\frac{L(t+1)}{L(t)} - \frac{K(t)}{L(t)} = s\left[\frac{K(t-\tau)}{L(t-\tau)}\frac{L(t-\tau)}{L(t)}\right]^{\alpha} - \delta\frac{K(t-\tau)}{L(t-\tau)}\frac{L(t-\tau)}{L(t)}.$$

Given that the labor force grows at a constant rate n,

$$\frac{L(t+1)}{L(t)} = 1 + n\text{and} \ \frac{L(t-\tau)}{L(t)} = (1+n)^{-\tau}.$$

The intensive capital accumulation equation incorporating the delay τ is expressed as

$$k(t+1) = \frac{1}{1+n}k(t) + \frac{s}{(1+n)^{1+\alpha\tau}}k^{\alpha}(t-\tau) - \frac{\delta}{(1+n)^{1+\tau}}k(t-\tau). \tag{7}$$

An another approach to incorporating a delay into the Solow model involves introducing a delay labor force as well. Specifically, if the labor input is subject to the same delay τ (i.e., production depends on $L(t-\tau)$), then the current output $Y(t)$ at time t is determined by the delayed inputs, $K(t-\tau)$ and $L(t-\tau)$. The corresponding intensive capital accumulation equation is given by

$$k(t+1) = \frac{1}{1+n}k(t) + \frac{s}{(1+n)^{1+\tau}}k^{\alpha}(t-\tau) - \frac{\delta}{(1+n)^{1+\tau}}k(t-\tau). \tag{8}$$

Compared to equation (7), equation (8) is only marginally simpler. However, identifying an economic scenario in which the delay in the labor force exactly matches the production delay of capital presents a significant challenge. If the delay in labor force differs from the production delay of capital, then the resulting capital accumulation equation incorporates two distinct delays, thereby increasing the complexity of the analysis. A thrid choice in which a delay is introduced directly into Equation (4) leads to a simplified capital accumulation:

$$k(t+1) = \frac{1}{1+n}k(t) + \frac{s}{1+n}k^{\alpha}(t-\tau) - \frac{\delta}{1+n}k(t-\tau) \tag{9}$$

Mathematically, Equation (9) does not differ significantly from Equation (7), however their economic implications are substantially different. As demonstrated in the derivation of Equation (7) from Equation (6), the dynamics of $k(t)$ governed by Equation (7) are inherently tied to the dynamics of $K(t)$ as described by Equation (6). The extensive capital accumulation equation derived from Equation (9) is given by

$$K(t+1) - K(t) = (1+n)^{\tau}\left[sK^{\alpha}(t-\tau)L^{1-\alpha}(t-\tau) - \delta K(t-\tau)\right].$$

The bracketed term represents net investment, defined as gross investment minus capital depreciation. The net change in the capital stock is given by gross investment multiplied by $(1+n)^{\tau}$ which exceeds unity when $n > 0$, equals to unity when $n = 0$ and fall below when $n < 0$. To further analyze Equation (9), it is necessary to justify the identical delay assumption mentioned earlier and appropriately modify the extensive capital accumulation equation.

Utilizing Equation (7). its corresponding steady-state expression is given by:

$$k_*^{\tau} = \left[\frac{s}{\left(n + \frac{\delta}{(1+n)^{\tau}}\right)(1+n)^{\alpha\tau}}\right]^{\frac{1}{1-\alpha}}.$$

It is evident that $k_*^{\tau} > 0$ for $n \geq 0$. Furthermore, the condition $k_*^{\tau} > 0$ also holds for $n < 0$ as the first factor in the denominator of k_*^{τ} remains positive. This follows from the inequality $1 > (1+n)^{\tau} > \delta$ or $\delta \geq (1+n)^{\tau}$ for $n < 0$ where, according to Assumption 1,

$$1 > \frac{\delta}{(1+n)^{\tau}} > \delta > -n \text{ or } \frac{\delta}{(1+n)^{\tau}} > 1 > \delta > -n.$$

To simplify subsequent analysis, we introduce the following assumption, which excludes excessively large values of τ when the population growth rate is negative[5]:

Assumption 2 In the case of $n < 0$, τ is restricted to values satisfying $(1+n)^{\tau+1} > \delta$.

Next, we analyze the stability of k_*^{τ}. To achieve this, we linearize equation (7) around the steady state, yielding an equation that explicitly incorporates the delay parameter τ:

$$k(t+1) - a_{\tau}k(t) + b_{\tau}k(t-\tau) = 0 \tag{10}$$

where for notational simplicity the deviation $k(t) - k_*$ is denoted as $k(t)$. The corresponding parameters are defined as follows:

$$a_{\tau} = \frac{1}{1+n} > 0 \tag{11}$$

[5] For $n = -1\%$, any τ satisfying $\tau > 229$ is eliminated when $\delta = 0.1$ and so is $\tau > 160$ when $\delta = 0.2$.

and

$$b_{\tau} = \frac{1}{1+n}\left[\frac{(1-\alpha)\,\delta}{(1+n)^{\tau}} - \alpha n\right]. \tag{12}$$

Since equation (10) is a $(\tau + 1)$th-order difference equation, its stability can be analyzed using the Rough-Hurwitz criterion.[6] However, as the value of τ increases, the complexity of the criterion grows, making it more challenging to apply. Nevertheless, Kuruklis (1994, Theorem 3) provides a comprehensive stability condition for the general case. Additionally, Papanicolan (1996) offers a more simplified set of necessary and sufficient conditions for the asymptotic stability of the difference equation (10), which are presented below:

Theorem 1 *The zero solution of equation (10) is asymptotically stable if and only if α_{τ} and b_{τ} belong to the interior of the set S:*

$$\begin{gathered}(i)\ \textit{when } \tau \textit{ is odd, the set } S \textit{ is constructed by } |a_{\tau}| - 1 < b_{\tau} \\ \textit{and the line segments of } \{(\pm\alpha(\theta),\ \beta(\theta))\}, \\ (ii)\ \textit{when } \tau \textit{ is even, the set } S \textit{ is constructed by } |b_{\tau} - a_{\tau}| = 1 \\ \textit{and the line segments of } \{(\pm\alpha(\theta),\ \pm\beta(\theta))\} \textit{ (same sign order)}\end{gathered}$$

where

$$\alpha(\theta) = \frac{\sin[(\tau+1)\theta]}{\sin(\tau\theta)} \textit{ and } \beta(\theta) = \frac{\sin(\tau)}{\sin(\tau\theta)} \textit{ for } 0 < \theta < \frac{\pi}{\tau+1}.$$

Figure 2 illustrates Theorem 1 for selected values of τ, specifically $\tau = 1, 3, 5, 7, 99$ in one case and $\tau = 2, 4, 6, 8, 100$ in the other: In Figure 2(A), the red boundary corresponding to $\tau = 1$ is an inverted isosceles triangle. The blue boundary for $\tau = 3$ is superimposed on it, followed sequentially by the green boundary for $\tau = 5$ and the black boundary for $\tau = 7$. The curved boundary for $\tau = 99$ represented by dotted black line passes through the points $(\pm 100/99, 1/99) \simeq (\pm 1, 0)$ where the straight line boundary intersects the horizontal axis. Similarly Figure 2(B) depicts the stability region boundaries for $\tau = 2$ (black); $\tau = 4$ (red); $\tau = 6$ (blue); $\tau = 8$ (green) with each boundary superimposed sequentially. The curved boundaries for $\tau = 100$ are illustrated as dotted black lines and pass through the points $(\pm 101/100, 1/100) \simeq (\pm 1, 0)$. Several key observations can be made. First, the stability region exhibits symmetry: it is symmetric with respect to the vertical axis in the (a_{τ}, b_{τ}) plane when τ is odd and symmetric with respect to the origin of the (a_{τ}, b_{τ}) plane when τ is even. Second, the size of the stability region decreases as τ increases. Third, as τ approaches infinity, the stability region converges to a square-diamond shape, regardless of whether τ is odd or even. Notably, the straight-line boundary intersects the curved segment at point $(\tau + 1/\tau, 1/\tau)$. For instance, the crossing points $(\pm 4/3, 1/3)$ for $\tau = 3$ are labeled in Figure 2(A), while the crossing points $(\pm 3/2, 1/2)$ for $\tau = 2$ are indicated in Figure 2(B). Additional crossing points are determined accordingly.

[6] See, for example, Gandorfo (1997).

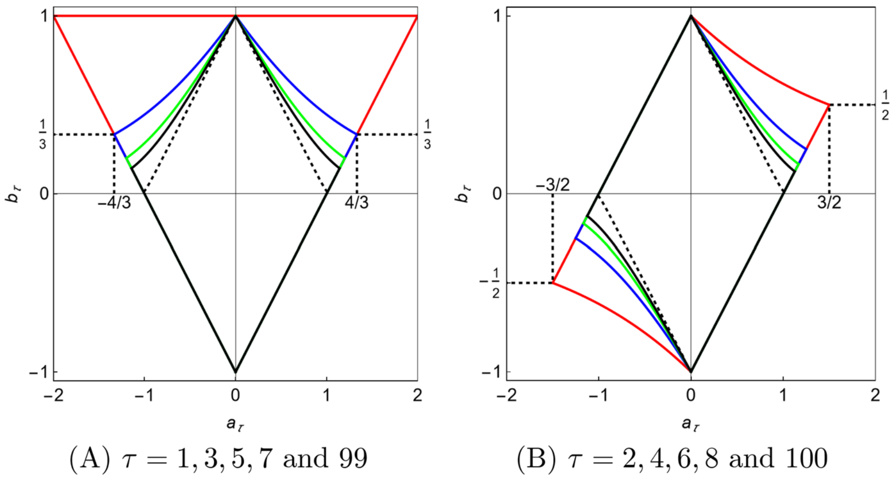

Fig. 2 Stability regions of equation (10) with various values

3.2 Stability regions with specific delay values

If the zero solution of the linearized equation (10) is asymptotically stable, then the corresponding positive steady state is locally absorbing. Conversely, the absence of asymptotic stability implies that nonlinear dynamics fully govern the behavior of the model. To explore these dynamics, we numerically verify the types of behavior that the nonlinear equation (7) can generate when the steady state loses its stability. Specifically, we assign a value of τ, construct the stability region according to Theorem 1 and examine the resulting dynamics within our discrete-time framework. As indicated in (11), we find that $a_\tau > 0$ for any τ; implying that only the right half of each stability region depicted in Figure 2 is relevant. For $\tau \geq 1$, we establish the following:

Theorem 2 *Under Assumptions 1 and 2,* $a_\tau > 0,\ a_\tau - 1 < b_\tau$ *and* $b_\tau < 1$ *hold for any* τ*.*

Proof The condition $a_\tau > 0$ follows directly from Equation (11). By substituting Equations (11) and (12), we obtain

$$1 + b_\tau - a_\tau = \frac{1-\alpha}{1+n}\left[\frac{\delta}{(1+n)^\tau} + n\right]$$

which remains positive for $n \geq 0$. In the case of $n < 0$, Assumptions 1 and 2 yield

$$\frac{\delta}{(1+n)^\tau} > \delta > -n,$$

implying that the bracketed term in the first equation is positive. Consequently, the inequality $a_\tau - 1 < b_\tau$ always holds. Next we examine $b_\tau < 1$,

$$b_\tau - 1 = -\frac{1}{1+n}\left\{(1+\alpha)n + \left[1 - \frac{(1-\alpha)\delta}{(1+n)^\tau}\right]\right\}$$

which is negative if $n > 0$ since $0 < (1-\alpha)\delta < 1$ and $(1+n)^\tau > 1$ ensuring that the bracketed terms in the above equation remain positive. For $n < 0$, the bracketed terms in the above equation can be rewritten as

$$b_\tau - 1 = -\frac{1}{1+n}\left\{(1+n)\left[1 - \frac{\delta}{(1+n)^{\tau+1}}\right] + \alpha\left[\frac{\delta}{(1+n)^\tau} + n\right]\right\}$$

which is negative since Assumptions 1 and 2 imply

$$1 - \frac{\delta}{(1+n)^{\tau+1}} > 0 \text{ and } \frac{\delta}{(1+n)^\tau} + n > 0.$$

Therefore, we conclude that $b_\tau < 1$ for any $\tau \geq 1$ regardless of the sign of n. □

We reconfirm the stability region of k_*^τ by specifying values of τ. We begin with $\tau = 1$ for which equation (7) is reduces to a quadratic form,

$$k(t+1) = \frac{1}{1+n}k(t) + \frac{s}{(1+n)^{1+\alpha}}k(t-1)^\alpha - \frac{\delta}{(1+n)^2}k(t-1). \quad (13)$$

The coefficients a_1 and b_1 in the corresponding characteristic equation are derived from Equations (11) and (12). It is well-known that the stability region is determined by the following three conditions,[7]

$$b_1 > -a_1 + 1,\ b_1 > a_1 - 1 \text{ and } b_1 < 1. \quad (14)$$

With $a_1 > 0$, these conditions define a triangular stability region, which corresponds to the right half of the inverse triangle in Figure 2(A). Theorem 2 directly implies the following result: the delay $\tau = 1$ is inconsequential, as any plausible pair of (a_1, b_1) lies within the stability region. These findings are summarized in the following corollary to Theorem 1:

Corollary 1 *Given Assumptions 1 and 2, the steady state of the quadratic equation (13) is asymptotically stable.*

Next we increase the value of τ to 2, resulting in Equation (7) becoming a cubic equation,

$$k(t+1) = \frac{1}{1+n}k(t) + \frac{s}{(1+n)^{1+2\alpha}}k^\alpha(t-2) - \frac{\delta}{(1+n)^3}k(t-2). \quad (15)$$

[7] See, for example, Gandolfo (1997).

The coefficients a_2 and b_2 of the corresponding cubic characteristic equation (10) are obtained from Equations (11) and (12). Farebrother (1973) provides simplified necessary and sufficient stability conditions for a cubic difference equation. Given that $a_2 > 0$, the following two conditions,

$$b_2 > a_2 - 1 \text{ and } b_2 < \frac{-a_2 + \sqrt{a_2^2 + 4}}{2}, \tag{16}$$

define the right half of parallelogram-like shape illustrated in black in Figure 2(B). Specifically, the stability region exhibits a triangular-like structure bounded by the vertical axis, the positively-sloped black straight line and the curved red segment which intersects the straight line at (3/2, 1/2). It is important to note that the final inequality in Equation (16) arises from the existence of a positive solution to $1 - a_2 b_2 - b_2^2 = 0$.

For convenience, we set $\alpha = 0.3$ and transform the stability region in the (a_τ, b_τ) plane to the corresponding stability region in the (n, δ) plane, as shown in Figure 3(A). The boundaries given by $1 - a_2 b_2 - b_2^2 = 0$ and $b_2 = a_2 - 1$ are, respectively, converted to

$$\delta = f_2(n) \equiv \frac{(1+n)^2}{7}\left(3n - 5\right) + \sqrt{5 + 8n + 4n^2}$$

and

$$\delta = g_2(n) \equiv -n(1+n)^2.$$

The equations $\delta = f_2(n)$ and $\delta = g_2(n)$ define, respectively, the positive-sloping and negative-sloping curves, both of which intersect at $(n_0^2, \delta_0^2) = (-1/3, 4/27)$. This point corresponds to the point (3/2, 1/2) in Figure 2(B). The negatively-sloped dotted black line is $\delta = -n$. Furthermore, Assumption 1 is violated in the light-green region, which is therefore excluded from further analysis.

We first derive the following results for $n \geq 0$. Solving $1 = f_2(n)$ yields $\bar{n}_2 \simeq 0.032$, while $g_2(n) < 0$ for $n > 0$; both of which imply that the steady state is asymptotically stable for $n > \bar{n}_2$. However, stability may be lost for $0 \leq n < \bar{n}_2$. More precisely, solving $\delta = f_2(n)$ with $n = 0.01 < \bar{n}_2$ results in a threshold value, $\delta_{H_2} \simeq 0.918$.[8] Next, we select δ as a bifurcation parameter and gradually increases its value from $\delta_1 = 0.8$ to $\delta_2 = 0.99$ along the vertical dotted line standing at $n = 0.01$ in Figure 3(A). Notice that point $(n, \delta_{H_2}) = (0.01, 0.981)$ lies on the upper boundary curve. The bifurcation diagram in Figure 3(B) illustrates the resulting dynamic behavior with respect to $\delta \in [\delta_1, \delta_2]$. The steady state, represented by the red segment remain stable for $\delta < \delta_{H_2}$ as it lies within the yellow (stability) region. In contrast, the the black dotted curve represents the unstable steady state and a cyclic motion emerges around the steady state through a super-critical Neimark-Sacker bifurcation when stability is lost for $\delta > \delta_{H_2}$ as it moves outside the yellow region.[9]

8 We refer to the meaning of this value shortly after.

9 We numerically confirm the occurrence of a super-critical bifurcation.

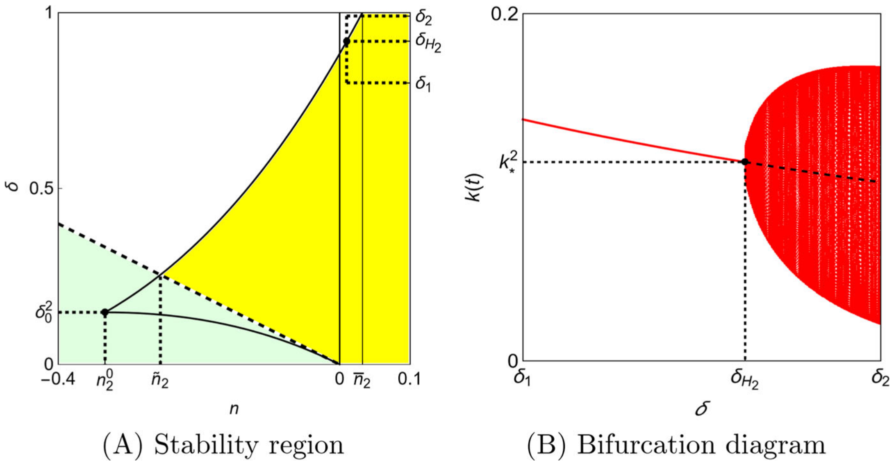

Fig. 3 Stability region and dynamics of $k(t)$ for $\tau = 2$

For $n < 0$, Assumption 1 is violated in the light-green region where $\delta \leq |n|$. For $0 \geq n \geq \tilde{n}_2 \simeq -0.255$, solving $\delta = f_2(n)$ determines the threshold value of δ at which stability is lost. Numerical results indicate that $\delta_{H_2} \simeq 0.849$ for $n = -0.01$ and $\delta_{H_2} \simeq 0.815$ for $n = -0.02$. Since the upper boundary has a positive-slop, the threshold value decreases as the absolute value of n increases in the negative direction. Once δ exceeds this threshold, stability is lost and a cyclic motion emerges around the steady state. These findings are summarized in the following (second) corollary to Theorem 1.

Corollary 2 *Given Assumptions 1 and 2, the steady state of equation (15) with $\tau = 2$ is asymptotically stable if $n \geq \bar{n}_2$; However for $n < \bar{n}_2$, the steady state loses stability at $\delta = \delta_{H_2}$, and undergoes a bifurcation leading to a limit cycle for $\delta > \delta_{H_2}$ where $\bar{n}_2$ solves $1 = f_2(n)$, while the threshold $\delta_{H_2} = f_2(n) < 1$ is specified for given values of $\tilde{n}_2 < n < \bar{n}_2$.*

In the case of $\tau = 3$, Eq. (7) is quartic,

$$k(t+1) = \frac{1}{1+n}k(t) + \frac{s}{(1+n)^{1+3\alpha}}k^{\alpha}(t-3) - \frac{\delta}{(1+n)^4}k(t-3) \tag{17}$$

and a_3 and b_3 of the corresponding characteristic equation are

$$a_3 = \frac{1}{1+n} \text{ and } b_3 = \frac{1}{1+n}\left[\frac{(1-\alpha)\,\delta}{(1+n)^3} - \alpha n\right].$$

Farebrother (1973) also provides simplified stability conditions for a quartic difference equation,

$$b_3 > a_3 - 1,\ \ b_3 < -a_3 - 1 \text{ and } (1-b_3)(1-b_3^2) - a_3^2 b_3 > 0.$$

Accordingly, the stability region corresponds to the right half of the diamond-shaped region in Figure 2(A) where the blue curved segment intersects the positively-sloped black straight line at the point (4/3, 1/3). The curved boundary is defined by one solution of b_3 of the cubic equation $(1-b_3)(1-b_3^2)-a_3^2 b_3=0$. Similar to the case of $\tau=2$, we set $\alpha=0.3$ and transform the stability region from the (a_τ, b_τ) plane to the region in the (n, δ) plane as shown in Figure 4(A). The curved boundary given by $(1-b_3)(1-b_3^2)-a_3^2 b_3=0$ and the straight boundary $b_3=a_3-1$ are, respectively, converted to

$$\delta = f_3(n) \equiv \frac{(1+n)^3}{42}\left[2(10+19n)+5\left(\frac{2^{4/3}(7+8n+4n^2)A}{B}+2^{2/3}\bar{A}B\right)\right]$$

with

$$A = 1 - i\sqrt{3} \text{ and } \bar{A} = 1 + i\sqrt{3},$$

$$B = \left[(1+n)\,(1+4n)\,(7+4n) + i3\sqrt{3}\sqrt{49+154n+205n^2+128n^3+32n^4}\right]^{1/3}$$

and

$$\delta = g_3(n) \equiv -n(1+n)^3.$$

The equations $\delta = f_3(n)$ and $\delta = g_3(n)$ describe the positive-sloping and negative-sloping curves, respectively, and intersect at $(n_3^0, \delta_3^0) = (-1/4, 27/256)$ in Figure 4(A). The intersection corresponds to the point (4/3, 1/3) in Figure 2(B). Similar to the case of $\tau=2$; Assumption 1 is violated in the light-green region. A comparison of Figures 3(A) and 4(A), reveals that a larger τ destabilizes the stability region, as an increase in τ shifts the upper boundary downward.[10] Consequently, the threshold value $\bar{n}_3 \simeq 0.087$, which solves $1 = f_3(n)$. Additionally, the other threshold value obtained by solving $\delta = f_3(n)$ for $n = 0.01$,[11] is $\delta_{H_3} \simeq 0.672$ which is lower than δ_{H_2}. The dynamics behavior generated by the quartic equation (17) is illustrated in Figure 4(B) for $\delta \in [\delta_1, \delta_2] = [0.6, 0.78]$. Qualitatively, the same results as those stated in Corollary 2 hold for $\tau = 3$.

For $\tau \geq 4$, a convenient analytical expression for the upper boundary of the stability region is not available. However, we refer back to Theorem 1 to determine the threshold values of δ. Specifically, we compute these thresholds under $\alpha = 0.3$ while n increasing in increments of 0.01 from -0.02 to 0.01:

We briefly summarize the results obtained in this section. The instability effect of delay is discussed because the intensive capital accumulation process without delay

[10] Although an increase of τ also shifts the lower boundary downward, the lower boundary is ineffective under Assumption 1.

[11] We also refer to the meaning of this value shortly after.

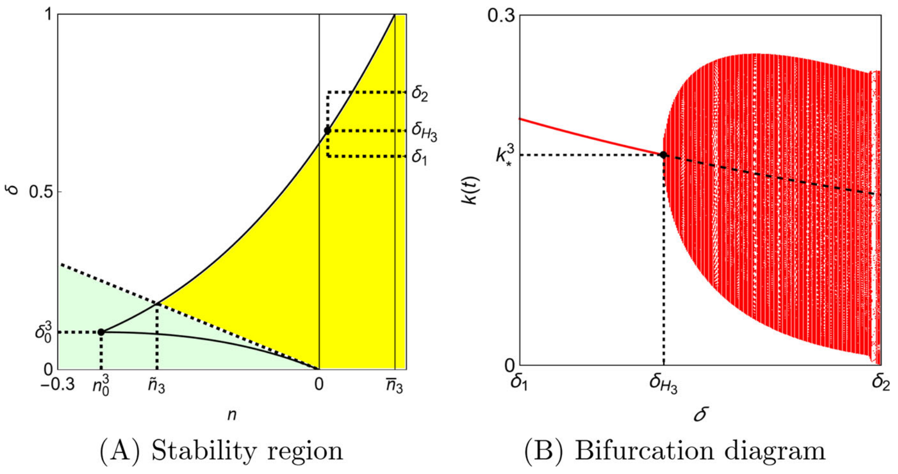

Fig. 4 Stability region and dynamics of $k(t)$ for $\tau = 3$

Table 1 Threshold values of δ_{H_τ} for various τ and n

	$n = -0.2\%$	$n = -0.1\%$	$n = 0\%$	$n = 0.1\%$
$\tau = 5$	0.340	0.372	0.407	0.443
$\tau = 10$	0.151	0.180	0.214	0.252
$\tau = 15$	0.086	0.112	0.145	0.185

is asymptotically stable. The linearized version of Eq. (4) evaluated at k_* is

$$k_d(t+1) = \frac{1}{1+n}\left[1 + \alpha(n+\delta) - \delta\right] k_d(t) \tag{18}$$

where $k_d(t) = k(t) - k_*$. The term $\alpha(n+\delta)$ is the production effect, δ is the depreciation effect and 1 is the trasition effect that conveys $k(t)$ to the next period. If we call $1-\delta$ the survival effect, then the stable Solow model without delay implies that the sum of the production and the survival effects is positive and less than $1+n$. In the same way, the linearized version of equation (7) evaluated at k_*^τ is

$$k_{d_\tau}(t+1) = \frac{1}{1+n}\left\{k_{d_\tau}(t) + [\alpha(n+\delta) - \delta]\, k_{d_\tau}(t-\tau) + D k_{d_\tau}(t-\tau)\right\} \tag{19}$$

with

$$D = (1-\alpha)\delta\left[1 - \frac{1}{(1+n)^\tau}\right]$$

where $k_{d_\tau}(t) = k(t) - k_*^\tau$. It is noticed that equation (19) is reduced to equation (18) for $\tau = 0$ since $D = 0$. Hence, the third term in the brackets of (19) denotes the effect caused by the positive delay. We call it the delay effect which is positive for $n > 0$ and negative for $n < 0$. The delay effect increases in absolute value as τ increases.

We have shown that the accumulation process with $\tau = 1$ is asymptotically stable, but the delay process with $\tau \geq 2$ loses stability and gives rise to cyclic fluctuation through a Neimark-Sacker bifurcation. Theorem 2 and Corollary 1 represent that the feasible paris of (a_τ, b_τ) are confined to the stability region with $\tau = 1$. Corollary 2 and the subsequent discussion suggest that the delay steady-state can be unstable for $\tau \geq 2$. As in a delay in a continuous-time system, a delay is harmless if it is small (i.e., $\tau = 1$) and harmful if it is large (i.e., $\tau \geq 2$).

As previously observed, the threshold values $\delta_{H_2} \simeq 0.918$ and $\delta_{H_3} \simeq 0.672$ for $\tau = 2$ and $\tau = 3$ with $n = 0.01$ are unusually high for depreciation rates, making it difficult to justify them within plausible economic context. Numerical results in Table 1 indicate that the destabilizing effect induced by increasing τ becomes more pronounced, leading to a decrease in the threshold value. Additionally, a lower population growth rate further accelerates this the destabilizing effect. It is worthwhile to extend the analysis of delay effects to similar growth models such as the Solow with a Constant Elasticity of Substitution (CES) production function studied by Sasaki (2019) or the semi-endogenous growth model examined by Christiaans (2011). In these frameworks, larger values of τ and smaller values of n may yield economically more plausible threshold values of δ which decline to be empirically relevant levels.

4 Two special cases

In this section, we introduce two key modifications to the dynamic equation (10). First, we decompose the delay into two distinct components and analyze the impact of each separately. Second, we reconsider the influence of delays when the labor force growth rate is negative, providing insights into how demographic decline interacts with delayed adjustments in the economic systems. These modifications offer a more comprehensive perspective on the role of delays in shaping long-run economic behavior.

4.1 No depreciation delay or no production delay

In this subsection, we distinguish between two types of time delays: one affecting changes in production, denoted as $k^\alpha(t - \tau_p)$, and the other influencing changes in depreciation, denoted as $\delta k(t - \tau_d)$. The first type, referred to as the production delay, $\tau_p \geq 0$, represents the time required for constructing and implementing new capital. The second type, known as the depreciation delay $\tau_d \geq 0$, accounts for the time needed to collect and process information regarding the depreciation of capital's economic value.[12] We begin with analyzing the effects of the production delay while assuming no depreciation delay. Under this assumption, Eq. (7) is modified as follows:

$$k(t+1) = \frac{1-\delta}{1+n}k(t) + \frac{s}{(1+n)^{1+\alpha\tau}}k^\alpha(t-\tau_p)$$

[12] It is possible that the production delay length is different from the depreciation delay length. See Matsumoto and Szidarovszky (2025) for justification for the two different delays.

where τ_P represents the production delay, and the steady state is modified to

$$k_*^{\tau_p} = \left[\frac{s}{(n+\delta)\,(1+n)^{\alpha\tau_p}} \right]^{\frac{1}{1-\alpha}}$$

which is positive under Assumption 1. The linearized equation is

$$k(t+1) = a_{\tau_p} k(t) + b_{\tau_p} k(t-\tau_p) \tag{20}$$

with

$$a_{\tau_p} = \frac{1-\delta}{1+n} \text{ and } b_{\tau_p} = \frac{\alpha(n+\delta)}{1+n}.$$

Assumption 1 implies

$$0 < a_{\tau_p} < 1 \text{ and } 0 < b_{\tau_p} < 1$$

and

$$a_{\tau_p} + b_{\tau_p} = 1 - \frac{(1-\alpha)(\delta+n)}{1+n} < 1$$

Clark (1976) demonstrates that the condition $a_{\tau_p} + \left|b_{\tau_p}\right| < 1$ given $0 < a_{\tau_p} < 1$ is a sufficient criterion for asymptotic stability. In our framework, the parameters a_{τ_p} and b_{τ_p} satisfy these conditions. a_{τ_p} is the survival effect and b_{τ_p} is the production effect. It is apparent form (20) that the steady-state $k_*^{\tau_p}$ is asymptotically stable if the production effect is zero or smaller than the survival effect in the sense of $b_{\tau_p} < 1 - a_{\tau_p}$. Consequently, a production delay alone does not destabilize the steady state. This result is formally stated as follows:

Theorem 3 *The production delay alone is inconsequential, and the steady state remains asymptotically stable for any* $\tau_p \geq 1$*, provided that* $\tau_d = 0$.

We now consider the reverse case and assume the absence of a production delay. Under this assumption, (7) is modified to

$$k(t+1) = \frac{1}{1+n} k(t) + \frac{s}{1+n} k^{\alpha}(t) - \frac{\delta}{(1+n)^{1+\tau}} k(t-\tau_d). \tag{21}$$

The corresponding steady state is

$$k_*^{\tau_d} = \left[\frac{s}{n + \frac{\delta}{(1+n)^{\tau_d}}} \right]^{\frac{1}{1-\alpha}}.$$

We implicitly assume that Assumption 2 also holds for τ_d, ensuring the existence of a positive steady state. The linearization of the system yields

$$k(t+1) = a_{\tau_d} k(t) - b_{\tau_d} k(t-\tau)$$

where

$$a_{\tau_p} = \frac{1}{1+n}\left[1+\alpha\left(n+\frac{\delta}{(1+n)^{\tau_d}}\right)\right] \text{ and } b_{\tau_d} = \frac{\delta}{(1+n)^{1+\tau_d}}.$$

By following the same procedure used to construct the stability regions in previous sections, we derive the stability regions for $\tau_d = 2$ and $\tau_d = 3$. These stability regions are then overlaid onto the existing stability regions from Figures 3(A) and 4(A) where $\tau = 2$ and $\tau = 3$, respectively. The results are illustrated in Figure 5(A) for $\tau_d = 2$ and Figure 5(B) for $\tau_d = 3$, both of which exhibit qualitatively similar outcomes. First, it is important to note that Assumption 1 is violated in the light-green regions. Second, in the presence of depreciation delay, the steady-state remains stable within the light-red region. Since the Solow model is inherently stable without delays, the stabilizing effect of the Solow framework outweighs the destabilizing effects introduced by depreciation delays within the light-red region. Furthermore, the effects of production delays are also evident. If a production delay is introduced ($\tau_p = \tau_d$), then the dynamic equation (21) reverts to equation (7) with $\tau_p = \tau_d$. Consequently, the yellow region is added to the light-red region, forming an expanded stability region in Figures 5(A) and 5(B). Within the yellow region, the depreciation delay introduces a destabilizing effect, while the production delay introduces a stabilizing effect. The latter dominates the former. leading to an overall expansion of the stability region. A comparison of these stability regions reveals that the size of the stability region negatively depends on the value of τ_d, indicating that an increase in depreciation delay has a destabilizing effect. In Figure 5(B), where the stability region for $\tau_d = 2$ is represented by dotted curves, it is evident that both the yellow and light red regions contract due to increasing depreciation delay. This implies that as τ_d increases, both stability regions shrink. These findings are formally summarized in the following theorem:

Theorem 4 *The stabilizing effect induced by the production delay dominates the destabilizing effect caused by the depreciation delay within the yellow region. However, as the overall delay increases, both effects cancel each other out, leading to a reduction in the size of the stability region.*

4.2 Negative population growth rate

As shown in Figure 1, some developed countries exhibit negative population growth rates, including Italy ($n = -0.08\%$), Hungary ($n = -0.28\%$), Japan ($n = -0.43\%$), Poland ($n = -1\%$), Latvia ($n = -1.14\%$). In this section, we analyze the long term economic evolution of these developed economies under condition of negative population growth. Even when $n < 0$, as long as Assumption 1 holds, asymptotic stability

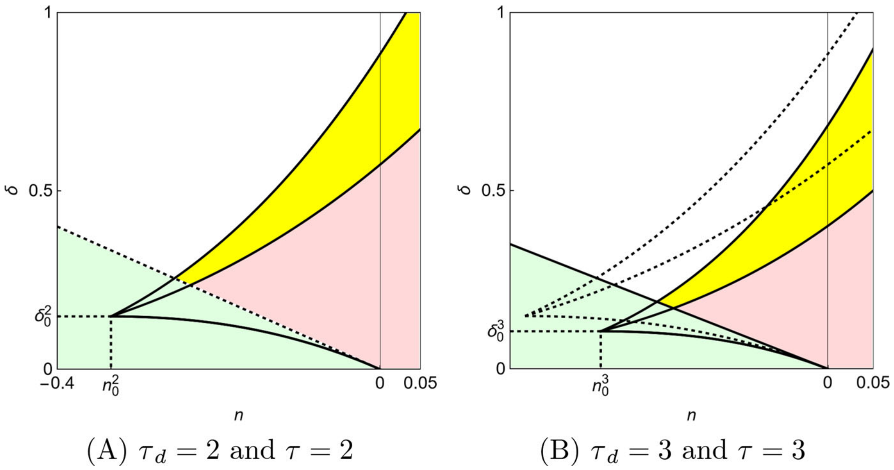

Fig. 5 Stabilizing effect of the production delay

remains preserved. Although the traditional Solow model does not explicitly consider policy interventions, many developed countries implement various economic policies and social security programs – such as pension systems, labor insurance, and child benefits - which can significantly influence long-term economic fluctuations. In particular, we examine the impact of child-rearing policies on long-run economic dynamics. Following Barro and Sala-i-Martin (2004, p.413) and Daitoh (2020, Sec. 3.1), we assume that child-rearing costs increase with parental wages, which are positively correlated with per-capita capital. For analytical simplicity, we further assume that child-rearing costs are proportional to per-capita capital, expressed as $\eta = ck(t)$. Since nL represents the number of births per unit time, the total expenditure on child-rearing is given by ηnL. Consequently, the extensive capital accumulation (6) is modified as follows:

$$K(t+1) - K(t) = sK(t-\tau)^{\alpha} L(t)^{1-\alpha} - \delta K(t-\tau) - \eta n L(t). \tag{22}$$

Consequently, the intensive capital accumulation equation is modified as follows:

$$k(t+1) = \frac{1}{1+n}\left[k(t) + \frac{s}{(1+n)^{\alpha\tau}}k(t-\tau)^{\alpha} - \frac{\delta}{(1+n)^{\tau}}k(t-\tau) - cnk(t)\right]. \tag{23}$$

The steady state under the child-rearing policy is given by

$$k_*^c = \left[\frac{s}{\left((1+c)n + \frac{\delta}{(1+n)^{\tau}}\right)(1+n)^{\alpha\tau}}\right]^{\frac{1}{1-\alpha}}.$$

Since k_*^c negatively depends on values of c, the introduction of a child-rearing program reduces the feasible parameter area. The positivity condition is given by

$$\delta > -(1+c)n(1+n)^{\tau}. \tag{24}$$

The linearized version of equation (23) evaluated at the steady-state is

$$k(t+1) = a_\tau^c k(t) - b_\tau^c k(t-\tau)$$

with

$$a_\tau^c = \frac{1-cn}{1+n} \text{ and } b_\tau^c = \frac{1}{1+n}\left[\frac{(1-\alpha)\delta}{(1+n)^\tau} - \alpha(1+c)n\right]$$

We assume that $\alpha = 0.3$ and $n = -0.1\%$. The threshold value of δ is determined by solving one of the stability conditions:

$$1 - a_2^c b_2^c - \left(b_2^c\right)^2 = 0 \text{ if } \tau = 2$$

and

$$\left(1 - b_3^c\right)^2 (1 + b_3^c) - \left(a_2^c\right)^2 b_3^c = 0 \text{ if } \tau = 3.$$

Hence, solving these equations along with $\delta = -(1+c)n(1+n)^\tau$ for different values of c (i.e., $c = 0$, $c = 20$, $c = 40$ and $c = 60$) yields the threshold values δ_τ^c and the lower boundary, $\bar{\delta}_\tau^c$:

$$\begin{cases} \delta_2^0 \simeq 0.948, \delta_2^{20} \simeq 0.693, \delta_2^{40} \simeq 0.545, \delta_2^{60} \simeq 0.406 \\ \bar{\delta}_2^0 \simeq 0.01, \bar{\delta}_2^{20} \simeq 0.206, \bar{\delta}_2^{40} \simeq 0.402, \bar{\delta}_2^{60} \simeq 0.598 \end{cases} \text{for } \tau = 2,$$

and

$$\begin{cases} \delta_3^0 \simeq 0.601, \delta_3^{20} \simeq 0.420, \delta_3^{40} \simeq 0.256, \ \delta_3^{60} \simeq 0.107 \\ \bar{\delta}_3^0 \simeq 0.01, \bar{\delta}_3^{20} \simeq 0.203, \bar{\delta}_3^{40} \simeq 0.398, \bar{\delta}_3^{60} \simeq 0.592 \end{cases} \text{for } \tau = 3.$$

The values corresponding to $c = 0$ represent the threshold value in the absence of child-rearing costs. For $n < 0$, δ_τ^c decreases as c increases; indicating a negative (i.e., destabilizing) effect of the child-rearing program. Conversely, $\bar{\delta}_\tau^c$ is increasing in c; demonstrating a positive effect that prevents the threshold value from decreasing excessively, thereby preserving the positive steady state. Figure 6(A) and 6(B) illustrate the trade-off associated with the child- rearing program: for $c = 20$, $c = 40$ and $c = 60$, the solid black, red and blue curves depict the negative effects, while the dotted curves of the same colors represent the positive effects. From these numerical results, we observe two key insights. First, a larger value of c lowers the threshold value of δ, increasing the likelihood of economic instability. Second, larger delays further amplify this risk, making economic instability more probable. Additionally, a

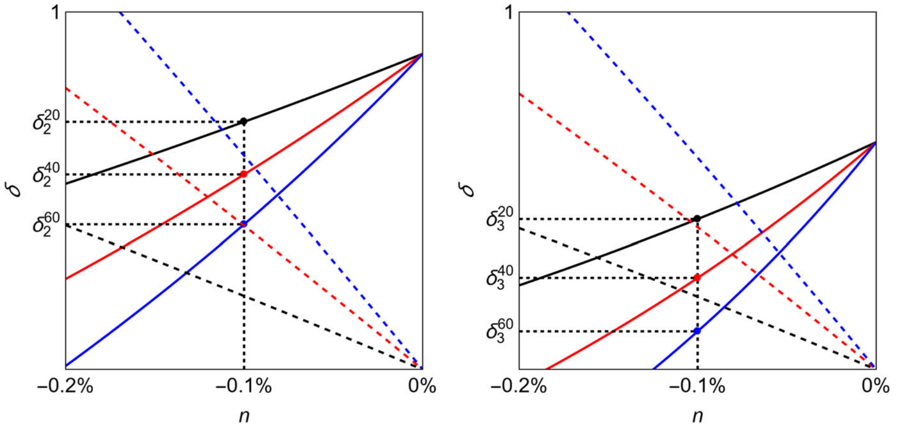

(A) $\tau = 2$ and $n = -0.1\%$ (B) $\tau = 3$ and $n = -0.1\%$

Fig. 6 Threshold values of δ when $n < 0$

higher c reduces the plausible region for the positive steady state. As a result of these opposing effects, we establish the following:

(i) $\delta_2^{60} < \bar{\delta}_2^{60}$ violates the positivity of k_*^c for $\tau = 2$,
(ii) $\delta_3^{40} < \bar{\delta}_3^{40}$ and $\delta_3^{60} < \bar{\delta}_3^{60}$ violate the positivity of k_*^c for $\tau = 3$.

For $\tau = 2$ and $n = -0.1\%$, the maximum feasible value the policy variable c lies between $c = 40$ and $c = 60$, suggesting that a plausible range for δ is $\delta_2^{40} < \delta < \delta_2^{60}$. Similarly, for $\tau = 3$ and $n = -0.1\%$, the maximum choice of c is constrained within the vicinity of δ_3^{20}. These results exhibit very strong sensitivity to parameter choices. If the growth rate is halved to $n = 0.05\%$, the feasible selection range for c or δ expands, whereas if the growth rate doubles, the range contracts. For economies with positive population growth rates, the child-rearing program contributes to economic stabilization. This is evidenced by the positive-sloping curves in Figure 6, which indicate that the instability regions shrink for $n > 0$. These findings are summarized in the following theorem:

Theorem 5 *The child- rearing program exerts a destabilizing effect in economies with $n < 0$ as it reduces the threshold value of δ, increasing the likelihood of economic instability.*

5 Delay solow model with non-constant $n(t)$

In standard growth theory, the labor force growth rate is typically assumed to be constant. However, this assumption implies an indefinitely expanding labor force, which is not a realistic representation of demographic trends. To address this limitation, we depart from the constant population growth rate assumption, and instead, introduce an autonomous difference equation to represent the dynamics of population growth:

$$n(t+1) = f\left[n(t)\right]. \tag{25}$$

Furthermore, we assume that equation (25) possesses at least one positive fixed point $n_* > 0$ such as $n_* = f(n_*)$. When the population growth rate is time-dependent, the intensive capital accumulation equation (7) must be accordingly modified. Dividing equation (6) by $L(t)$ yields

$$\frac{K(t+1)}{L(t+1)}\frac{L(t+1)}{L(t)} - \frac{K(t)}{L(t)}$$
$$= s\left[\frac{K(t-\tau)}{L(t-\tau)}\prod_{i=1}^{\tau}\frac{L(t-i)}{L(t-(i-1)))}\right]^{\alpha} - \delta\frac{K(t-\tau)}{L(t-\tau)}\prod_{i=1}^{\tau}\frac{L(t-i)}{L(t-(\tau-(i-1)))}$$

which is rewritten as

$$k(t+1) = \frac{1}{1+n(t)}\left[k(t) + \frac{s}{[N(\boldsymbol{n})]^{\alpha}}k^{\alpha}(t-\tau) - \frac{\delta}{N(\boldsymbol{n})}k(t-\tau)\right] \tag{26}$$

where

$$N(\boldsymbol{n}) = \prod_{i=1}^{\tau}(1+n(t-i)) \text{ with } \boldsymbol{n} = (n(t-1), n(t-2), ..., n(t-\tau)),$$

$$\frac{L(t+1)}{L(t)} = 1 + n(t) \text{ and } \frac{L(t-i)}{L(t-(i-1))} = [1+n(t-i)]^{-1}.$$

Equation (26) is a $(\tau+1)$th order difference equation incorporating non-constant population growth rates, $n(t-i)$ for $i = 0, 1, 2, ..., \tau$. This equation characterizes the evolution of per-capita capital over times. For $n(t) = n_*$ for all t, the steady state of Equation (26) is given by

$$k_{**}^{\tau} = \left[\frac{s}{\left(n_* + \frac{\delta}{(1+n)^{\tau}}\right)(1+n_*)^{\alpha\tau}}\right]^{\frac{1}{1-\alpha}}.$$

To facilitate dynamic analysis, we consider specific equations. In the simplest case of $\tau = 1$, Equation (26) simplifies to:

$$k(t+1) = \frac{1}{1+n(t)}\left[k(t) + \frac{s}{[1+n(t-1)]^{\alpha}}k^{\alpha}(t-1) - \frac{\delta}{1+n(t-1)}k(t-1)\right]. \tag{27}$$

Equations (25) and (27) together form a higher-order system, which can be transformed into a first-order four-dimensional (4D) system. This system characterizes the dynamics of the steady state k_{**}^1 and the associated variables,

$$\begin{cases} k(t+1) = \dfrac{1}{1+n(t)}\left[k(t) + \dfrac{s}{(1+w(t))^{\alpha}}x^{\alpha}(t) - \dfrac{\delta}{(1+w(t))}x(t)\right], \\ x(t+1) = k(t), \\ n(t+1) = f\left[n(t)\right], \\ w(t+1) = n(t). \end{cases} \tag{28}$$

It is important that the per-capita capital negatively depends on the population growth rate, while the labor force growth rate remains self-contained. This one-way dependency simplifies the dynamic analysis and serves as a useful starting point to consider dynamics of the high-dimensional system. The steady-state value also exhibits a positive dependence on the saving rate, and a negative dependence on the depreciation rate. Additionally, the fourth equation of $w(t+1) = n(t)$ in Equation (28) can be replaced with $w(t+1) = f[w(t)]$ since

$$w(t+1) = n(t) = f\left[n(t-1)\right] = f[w(t)].$$

To analyze the stability of the steady-state, we linearize nonlinear system (28) incorporating $w(t+1) = f[w(t)]$ in the neighborhood of the steady state,

$$z(t+1) = \boldsymbol{J}z(t)$$

where $z(t) = (k(t) - k_*, x(t) - k_*, n(t) - n_*, w(t) - n_*)^T$ is a column vector representing deviations from the steady state, and $\boldsymbol{J}$ denotes the coefficient matrix (i.e., the Jacobian matrix) of system (28),

$$\boldsymbol{J} = \begin{pmatrix} a_1 & -b_1 & c_n & c_w \\ 1 & 0 & 0 & 0 \\ 0 & 0 & f_n & 0 \\ 0 & 0 & 0 & f_w \end{pmatrix}$$

with a_1 and b_1 being defined in (11) and (12),

$$c_n = \frac{\partial k(t+1)}{\partial n(t)}, \; c_w = \frac{\partial k(t+1)}{\partial w(t)}, \; f_n = \left.\frac{df}{dn}\right|_{n=n_*} = f_w \left.\frac{df}{dw}\right|_{w=w_*} = f_*$$

The characteristic equation of the coefficient matrix is

$$|\boldsymbol{J} - \lambda \boldsymbol{I}| = (f_* - \lambda)^2(\lambda^2 - a_1\lambda + b_1) = 0. \tag{29}$$

According to Corollary 1, the quadratic polynomial of the second factor in Equation (29) yields two eigenvalues with absolute values less than unity. Consequently. the stability of the steady state depends on the value of f_* which, in turn, is determined by the specification of the population law function, $f(n)$. The steady state is locally asymptotically stable if $|f_*| < 1$ and becomes unstable otherwise.

For $\tau = 2$, equation (26) with a non-constant population growth rate $n(t)$ is modified as follows:

$$k(t+1) = \frac{1}{1+n(t)}\left[k(t) + \frac{s}{[N(n(t-1), n(t-2))]^{\alpha}}k^{\alpha}(t-2) - \frac{\delta}{N(n(t-1), n(t-2))}k(t-2)\right]$$

with

$$N(n(t-1), n(t-2)) = (1+n(t-1))\,(1+n(t-2))$$

By analogy with the $\tau = 1$ case, it is straightforward to derive the following form of the characteristic equation:

$$(f_* - \lambda)^3(\lambda^3 - a_2\lambda^2 + b_2) = 0.$$

Corollary 2 implies that the threshold value of the cubic equation is approximately $\delta_{H_3} \simeq 0.672$. Under natural circumstances, the actual depreciation rate is likely to be lower than δ_{H_3}, in which case, the stability of the steady state once again depends on the slope of $f(n)$ at the equilibrium population growth n_*. As the value of τ increases, the dynamic system becomes more complex. However, its stability remains contingent on f_*. The stability and instability of the Solow model with a time-dependent population growth rate $n(t)$ is highly sensitive to the specification of $f(n)$. Maynard (1974) identifies two key properties of a realistic population growth model:

1) The population grows at a constant growth rate when its size is sufficiently small.
2) The population growth rate declines to zero as the population size becomes larger.

In the field of population dynamics, it is well established that the logistic map in continuous time satisfies these properties. Verhulst (1845) was the first to employ the logistic map to analyze population dynamics as an extension of the exponential (i.e., constant rate) population growth. Accinelli and Brida (2005) introduce a generalized logistic equation also known as Richards' equation, to model population growth. Although their study is conducted in a continuous-time framework, its discrete-time counterpart in our notation can be expressed as follows:

$$f\left[n(t)\right] = (1+r)n(t)\left[1 - (n(t))^{\sigma}\right] \tag{30}$$

The parameter σ serves as a shape parameter that introduces asymmetry into the population growth function. Brianzoni et al. (2007) assume the Beverton-Holt equation for $f(n)$ since the discrete-time Beverton-Holt equation is thought to be equivalent to the continuous-time logistic equation.[13] Tramontana et al. (2015) assume the original

[13] The Beverent-Holt equation and the logistic equation are

$$f(n(t)) = \frac{rn(t)}{1+(r-1)n(t)/M} \text{ and } \frac{dL}{dt} = r\left(1 - \frac{L}{M}\right)$$

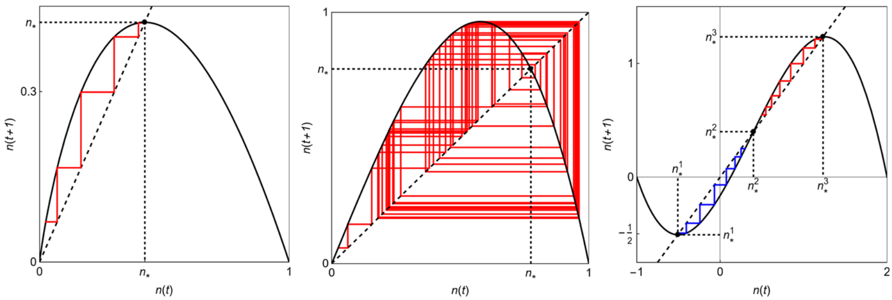

(A) $\sigma = 1/3,\ r = 3$ (B) $\delta = 2,\ r = 3/2$ (C) Cubic function

Fig. 7 Various forms of $n(t+1) = f[n(t)]$

logistic equation, that is, equation (30) with $\sigma = 1$. When $\sigma = 1$, the logistic curve is symmetric around the vertical line at $n = 1/2$. However, when $\sigma \neq 1$, this symmetry is distorted. In particular, if $\sigma < 1/2$, the peak of the curve shifts leftward, conversely, if $\sigma > 1/2$, the peak shifts rightward. Figure 7(A) illustrates the case where the function $n(t+1) = f\,[n(t)]$ is plotted for $\sigma = 1/3$ and $r = 3$. In this scenario, the trajectory of $n(t)$ monotonically converges to a positive steady state. In contrast, Figure 7(B) depicts the function for $\sigma = 2$ and $r = 3/2$, where the emergence of complex dynamics results in fluctuations around the steady state. In Figure 7(C), the functional form of $f(n)$ is extended to a cubic equation, introducing both a maximum and a minimum.[14] The dynamics become highly sensitive to initial conditions as follows. If the initial value of $n(0)$ exceeds the middle steady-state, n_*^2, the trajectory converges to the upper steady-state n_*^3. Conversely, if $n(0) < n_*^2$, the trajectory converges to a negative steady-state n_*^1. Thus, the middle steady-state represents a critical threshold that determines whether a country's population stabilizes in prosperity or declines towards stagnation. Needless to say, as the nonlinearity of this cubic equation intensifies, even more complicated dynamics behaviors may arise near the lower and upper steady-states.

6 Concluding remarks

This study has developed a delay Solow model within a discrete-time framework. We derive an intensive (i.e., per-capita) capital accumulation equation under the standard assumption of a positive constant population growth rate and construct the stability region of the steady-state in the presence of delays.

First, we demonstrate that the delayed Solow model can generate cyclic fluctuations through a Neimark-Sacker bifurcation when the depreciation rate exceeds a critical threshold, beyond which stability is lost. This threshold value is positively correlated

---

where r is the proliferation rate and M is the environmental carrying capacity. Explicit solutions of these equations are

$$n(t) = \frac{Mn_0}{n_0 + (M - n_0)r^{-t}} \text{ and } L(t) = \frac{ML_0}{L_0 + (M - L_0)e^{-rt}}.$$

[14] Actually, $f(n) = -0.65(n+1)(n-1/8)(n-2)$.

with the length of delay and negatively correlated with the population growth rate, indicating that cyclical solutions in the delayed difference equation are more likely to emerge when the delay is prolonged and the growth rate is lower. Second, we distinguish between two types of delays: production delays and depreciation delays. Our analysis confirms that production delays do not affect stability, whereas depreciation delays have a destabilizing effect on the economy. Third, we examine the impact on economic growth from child security policies implemented in developed or "rich" countries experiencing diminishing or negative population growth rates. Specifically, we analyze child-rearing programs and demonstrate such expenditures act as a destabilizing factor in economic growth, as they reduce the threshold value of the depreciation rate. Finally, we extend the model by replacing the constant population growth rate with a non-constant growth function. Our finding indicate that the dynamics of economic growth are highly sensitive to the specification of the autonomous population law function.

For analytical simplicity we assume that production and depreciation delays are identical. A natural extension of this work would be to examine how differing delays influences economic growth dynamics. Additionally, while we adopt the Cobb-Douglas production function for tractability, an interesting topic for future research is to replace it with a Constant Elasticity of Substitution (CES), particularly in cases where the elasticity of substitution is less than unity. Furthermore, extending the model by modifying the function $f(n)$ to $f(n, k)$ is a promising direction, although the associated stability analysis presents significant challenges.

Funding Open access funding provided by Corvinus University of Budapest.

References

Accinelli, E., Brida, G.: Re-formulation of the Solow economic growth model whit the Richards population growth law, GE, Growth, Math methods 0508006, University Library of Munich, Germany

Barro, R., Sala-i-Martin, X.: Economic Growth, 2nd edn. MIT Press, Cambridge, London (2004)

Brianzoni, S., Mammana, C., Michetti, E.: Nonlinear dynamics in a business-cycle model with logistic population growth. Chaos, Solitons Fractals **40**, 717–730 (2009)

Brianzoni, S., Mammana, C., Michetti, E.: Complex dynamics in the neoclassical growth model with differential savings and non-constant labor force growth. Stud. Nonlinear Dyn. Econom. **11**, 3 (2007)

Braida, J., Pereyra, J.: The Solow model in discrete time and decreasing population growth rate. Econ. Bull. **3**, 1–14 (2008)

Christiaans, T.: Semi-endogeneous growth when population is decreasing. Econ. Bull. **31**, 2667–2673 (2011)

Clark, C.: A delay-recruitment model of population dynamics with an application to baleen whale populations. J. Math. Biol. **3**, 381–391 (1976)

CIA The World Factbook, Population Growth Rate Comparison and Population Comparion, URL: https//www.cia.gov/the-world-facebook/field/, (2024)

Daitoh, I.: Rates of population decline in solow and semi-endogeneous growth models: emprical relevance and the role of child rearing cost. Int. Econ. **23**, 218–234 (2020)
Day, R.: Irregular growth cycles. Am. Econ. Rev. **72**, 406–414 (1982)
Farebrother, R.: Simplified Samuelson conditions for cubic and quartic eautaions. Manch. Sch. Econ. Soc. Stud. **41**, 396–400 (1973)
Gandolfo, G.: Economic Dynamics, Study Edition. Springer-Verlag, Berlin, Heidleberg (1997)
Guerrini, L., Matsumoto, A., Szidarovszky, F.: Neoclassical growth model with two fixed delays. Metroeconomics **79**, 423–441 (2019)
Kalecki, M.: A macroeconomic theory of business cycles. Econometrica **3**, 327–344 (1935)
Kydland, F., Prescott, E.: Time-to-Build and aggregate fluctuations. Econometrica **50**, 1345–70 (1982)
Kuruklis, S.: The asymptotic stability of $x_{n+1} - ax + bx_{n-k} = 0$. J. Math. Anal. Appl. **188**, 719–731 (1994)
Matsumoto, A., Szidarovszky, F.: Delay Solow model revisited, to appear in Metroeconomics, (2025)
Matsumoto, A., Szidarovszky, F.: Delay Solow model with a normalized CES production function. J. Econ. Behav. Organ. **213**, 305–323 (2023)
Maynard, J.: Models in Ecology. Cambridge University Press, Cambridge (1974)
Papanicolaou, G.: On the asymptotic stability of a class of linear difference equations. Math. Mag. **69**, 34–43 (1996)
Sasaki, H.: The Solow growth model with a CES production function and declining population. Econ. Bull. **39**, 1979–1988 (2019)
Solow, R.: A contribution to the theory of economic growth. Quarterly Journal of Economics **70**, 65–94 (1956)
Tramontana, F., Sushko, I., Aviutin, V.: Period adding structure in a 2D discontinuous model of economic growth. Appl. Math. Comput. **253**, 263–273 (2015)
Verhulst, P.: Recherches math ematiques sur la loi d'accroissement de lapopulation. Nouveaux m emoires de l'acad emie royale des sciences et belles-lettres deBruxelles **18**, 1–38 (1845)
World Population Prospects (2024), https://www.population.un.orgwpp/assets/, URL:Files/WPP2024.Summary-of-Results.pdf
Zak, P.: Kaleckian Lags in General Equilibrium. Rev. Polit. Econ. **11**, 321–330 (1999)